

Understanding Anisotropy and Architecture in Ice Templated Biopolymer Scaffolds

K. M. Pawelec, A. Husmann, S. M. Best, R. E. Cameron

July 11, 2013

Biopolymer scaffolds have great therapeutic potential in the field of tissue engineering due to the large interconnected porosity and natural biocompatibility of the polymers. Using an ice templated technique, where collagen is concentrated into a porous network by ice nucleation and growth, scaffolds with anisotropic pore architecture can be created, mimicking natural tissue environments such as tendon or cardiac muscle. This paper describes a systematic set of experiments which have been undertaken to understand the effects of local temperature control on the anisotropy and architecture of ice templated biopolymer scaffolds. The scaffolds within this study were at least 10 mm in all dimensions, making them applicable to critical sized defects for biomedical applications. It was found that monitoring the temperature within slurry at specific locations during freezing was critical to predicting anisotropy of scaffold architecture. Aligned porosity was produced only when the temperature at nucleation was above the equilibrium freezing temperature (0 °C) in parts of the slurry volume. Thus, the key to creating scaffold anisotropy is that the local cooling rates within the liquid slurry are sufficiently different to ensure that freezing equilibrium temperature is not reached throughout the slurry volume at nucleation. This principal was valid over a range of collagen slurries, for the first time demonstrating that by monitoring the temperature within slurry during freezing, scaffold anisotropy with ice templated scaffolds can be predicted.

1 Introduction

The focus of tissue engineering is to create environments which encourage cells to heal damaged tissue without a loss of functionality. While work has been done to elucidate and replicate the chemical environment in which cells reside, less is known about how architectural cues affect cells. However, a growing body of evidence suggests that three-dimensional scaffold structures may be critical to induce cellular organization and replicate anisotropic tissues, such as muscle [1].

Freeze drying is one highly versatile technique used to create scaffolds with architectures ranging from pore size distributions, aligned, and even radial pore structures [2, 3, 4, 5]. During the freeze drying process, which consists of freezing a water based suspension then removing the ice via sublimation, scaffold architecture is determined by ice crystal growth. As the ice crystals grow, they push aside the solid phase, consisting of large polymer chains and smaller solutes, concentrating it in the volume between the growing crystals. Once the ice is subsequently removed, only a porous skeleton is left which mirrors the ice structure. Thus, the scaffold architecture produced is limited to structures which can be created by ice nucleation and growth.

Scaffold architecture is directly related to where and when ice nucleation occurs, as nucleation is the key step of the freezing process [6, 7]. As the first step in solidification, nucleation is a stochastic process,

which can occur globally throughout the entire volume, or locally in specific regions of the sample, leading to anisotropic crystal structures[8]. In order to offset the decrease in entropy accompanying the transition from a liquid to a solid, the formation of primary nuclei does not occur at the equilibrium freezing temperature, 0 °C for the ice-water system, but at temperatures below equilibrium [9, 10]. The formation of stable nuclei is accompanied by latent heat release which brings the temperature back to the equilibrium freezing temperature, whereupon crystal growth takes over [9].

The freeze drying process has many parameters which can be controlled to influence ice nucleation and growth, reflected in the final scaffold pore structure. It is important to note that a change in processing parameters does not translate directly to a change in the local thermal events within the suspension, as demonstrated by O'Brien et al[11]. Variables which can be controlled are termed 'set' variables and include: set freezing temperature, set cooling rate, and mold design. While set freezing temperature and moderate changes to set cooling rate, between 0.6 - 4.1 °C/min, can change pore size, they cannot induce anisotropic structures [12, 13]. However, radically altering the cooling rate, such as quenching with liquid nitrogen, can change where nucleation occurs and lead to anisotropic pore structures [14]. While set parameters have been explored to produce scaffolds with varying architecture, surprisingly little attention has been given to relating local thermal events, such as nucleation temperature, freezing time and cooling rate, to scaffold structure.

This study sought to understand the local changes in thermal parameters during freezing of collagen slurries and use them to predict microstructure. We hypothesized that monitoring the local thermal behavior of slurry during freezing would provide the underlying principal responsible for scaffold anisotropy, and lead to a more robust way to predict scaffold anisotropy than the manipulation of external set parameters. As far as we are aware, this is the first systematic investigation into the underlying mechanisms leading to scaffold architecture in collagen slurry. With greater understanding of the mechanisms controlling scaffold architecture, more complex tissue engineered constructs should be possible, a significant step towards mimicking the in vivo environment.

2 Materials and Methods

2.1 Scaffold Production

Suspensions of 1 wt% and 0.5 wt% collagen were prepared by hydrating bovine Achilles tendon, type I collagen (Sigma Aldrich) in 0.05M acetic acid, adjusted to pH 2. Slurries were homogenized at 13,500 rpm for 30 minutes in an ice water bath (VDI 25, VWR International Ltd, UK), and centrifuged (Hermle Z300) for 5 minutes at 2500 rpm.

Prepared suspensions were poured into a perspex mold with a standard cylindrical shape: inside diameter of 22 mm and a height of 30 mm, Figure 2. As perspex has a similar thermal diffusivity to water (within 25%), the mold was designed to have thick outer walls to ensure that a radial temperature gradient was established within the mold walls and not the slurry [15, 16]. Therefore, within the slurry, only axial temperature gradients were generated. In this way, the filling height of the slurry was the only factor affecting the temperature gradients produced within the slurry volume. This was verified by a first order simulation of the conductive cooling, and is illustrated schematically in Figure 1. Temperature measurements made at each point in the slurry were thus representative of bulk at a specific filling height. During the study, the filling height was varied from 5, 10, 15, and 20 mm, corresponding to volumes of 1.9, 3.8, 5.7, and 7.6

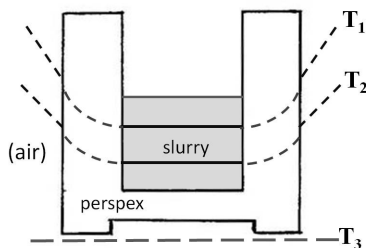


Figure 1: Schematic of the thermal profiles within the air, perspex mold, and collagen slurry. The thermal conductivity of the mold results in purely axial gradients within the slurry during cooling, labeled T_1 and T_2 . The shelf temperature (T_3), is the minimum temperature within the system: $T_3 < T_2 < T_1$. Thus thermal measurements made within the slurry at the mold edges were representative of the freezing behavior at the center of the slurry as well.

ml respectively. The slurry was cooled, at a rate of $0.9\text{ }^\circ\text{C}/\text{min}$, to $-30\text{ }^\circ\text{C}$ and held for 90 minutes, then lyophilized using a Virtis freeze drier (SP Industries, USA) at $0\text{ }^\circ\text{C}$ for 20 hours under a vacuum of less than 100 mTorr.

2.2 Scanning Electron Microscopy

All scanning electron microscopy images were taken using a JEOL 820, with a tungsten source, operated at 10 kV. Cross-sections of the collagen scaffolds were sputter coated for 2 minutes with platinum, at a current of 40 mA prior to imaging. Micrographs from two separate scaffolds were compared to verify reproducibility.

2.3 Pore Size Analysis

Pore size analysis was performed on scaffold images obtained via X-ray micro-tomography (Skyscan 1072). Scans were taken at a magnification of 75x, with a voltage of 25kV, current of $132\mu\text{A}$, and exposure time of 7.5 seconds. Reconstructions were performed with the software program NRecon, part of the Skyscan system. Average pore size was determined by line-intercept method. After verifying that the scaffold had consistent pore architecture via scanning electron microscopy, twelve sections from each scaffold were analyzed, with three lines per image. Pore size analysis was only done on scaffolds which had isotropic, equiaxed pore architecture.

2.4 Thermal Characterization

The Virtis freeze drier (SP Industries, USA) was equipped with thermocouples, which were positioned at the base and top of the slurry. Temperature measurements were recorded every 10 seconds during suspension freezing. Set cooling rate refers to the cooling rate of the shelf-ramping lyophilizer; final set freezing temperature refers to the set temperature of the shelf during the freezing cycle, Figure 2.

From the thermal curves at the top and base of the slurry, several parameters were obtained: nucleation temperature, cooling rate of the slurry, and freezing time. Nucleation temperature was defined as the temperature which the slurry reached before latent heat release caused the temperature to jump back to equilibrium. If thermal curves did not display the characteristic jump to the equilibrium freezing temperature, no nucleation temperature was recorded at that site. Freezing was considered to be initiated when the nucleation temperature was reached, or, if no nucleation occurred, freezing was considered to be initiated

when the thermal curve crossed the equilibrium freezing temperature. The end of freezing was defined as the extrapolated point at which the initial slope of the thermal line changed. Freezing time was measured between these two points. Figure 2 illustrates the parameters measured.

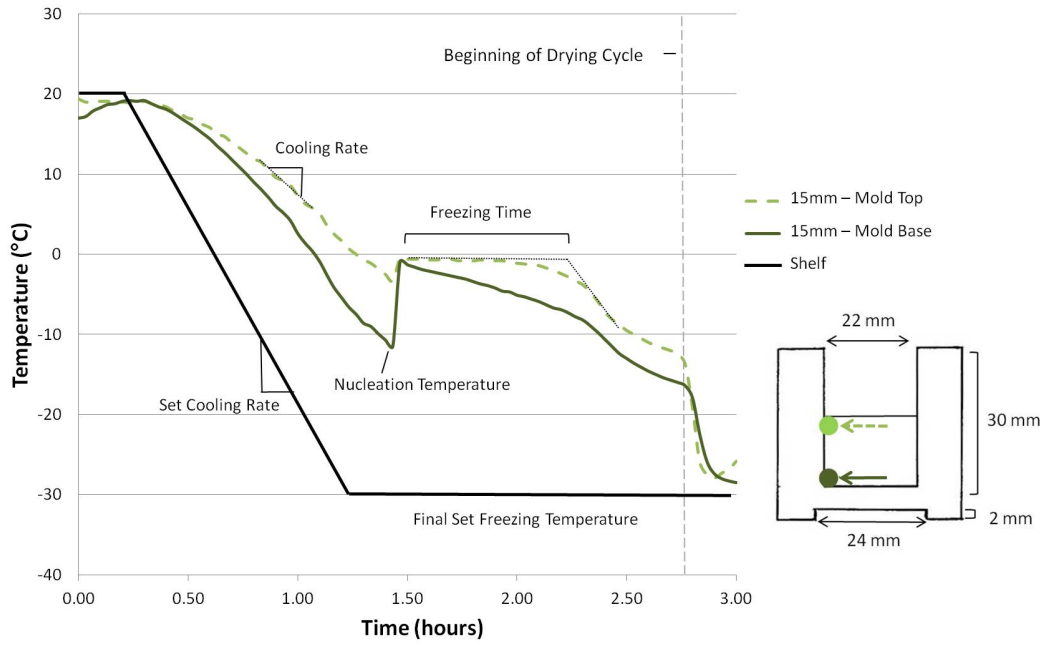


Figure 2: A representative thermal profile within a collagen slurry during freezing, with the quantified freezing parameters labeled, and a schematic of the freeze drying mold used throughout the study.

2.5 Statistics

For each filling volume, a sample size of 3 was used. Groups were compared via Student's t with a confidence interval of 95%.

3 Results

3.1 Thermal Profile Features

Thermal curves at top and base were sensitive to variations in filling height, Figure 3. In all cases, regardless of filling height or collagen weight percentage, it appeared that the nucleation was driven by the base of the mold. Once the base nucleated, releasing latent heat, neither the base or the top of the slurry appeared to nucleate again. A temperature gradient was established before and after nucleation, as the base cooled more quickly than the top of the slurry.

3.2 Effect of Filling Height

Filling height affected all of the thermal parameters measured, and the trends were consistent between slurries with different weight percentages of collagen. Freezing time, at both the top and the base of the

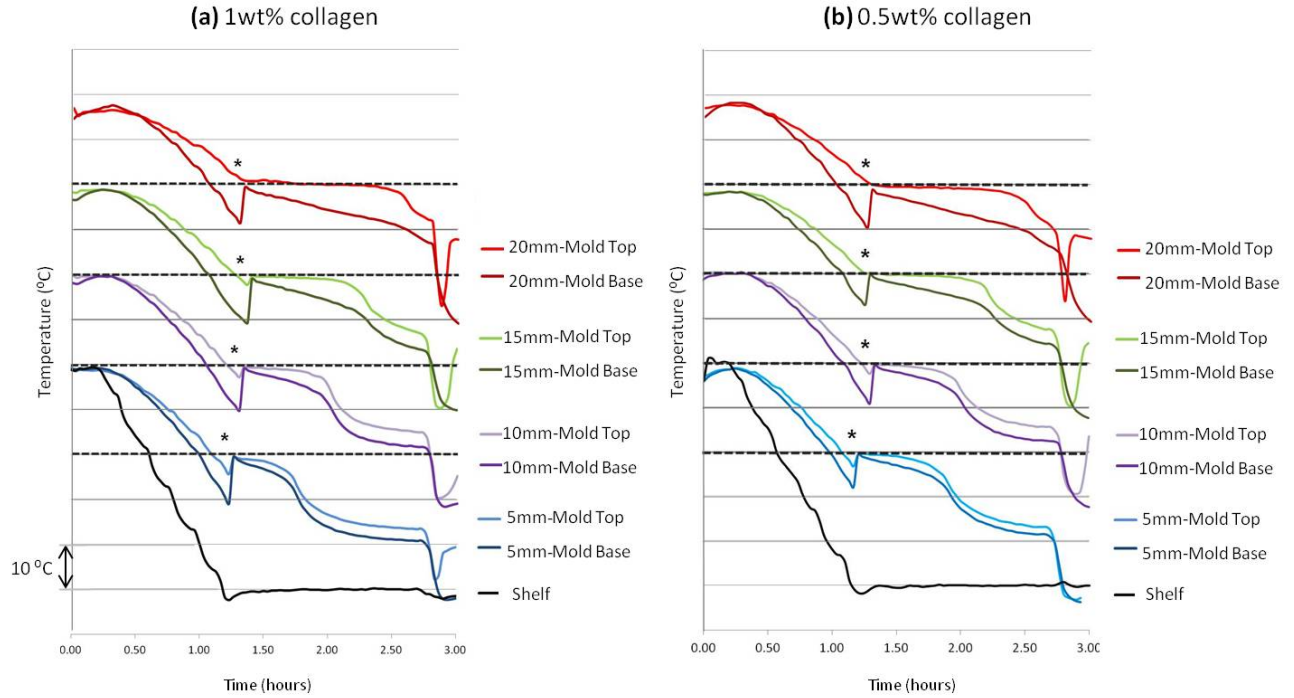


Figure 3: Thermal profiles as a function of filling height for (a) 1 wt% collagen scaffolds and (b) 0.5 wt% collagen scaffolds. The profiles illustrate the changes, particularly in freezing time and nucleation temperature, at the top and base of the slurry. Each interval on the temperature axis represents a change of 10 °C; bold dashed lines indicate 0°C for each set of thermal profiles. *Latent heat release at nucleation.

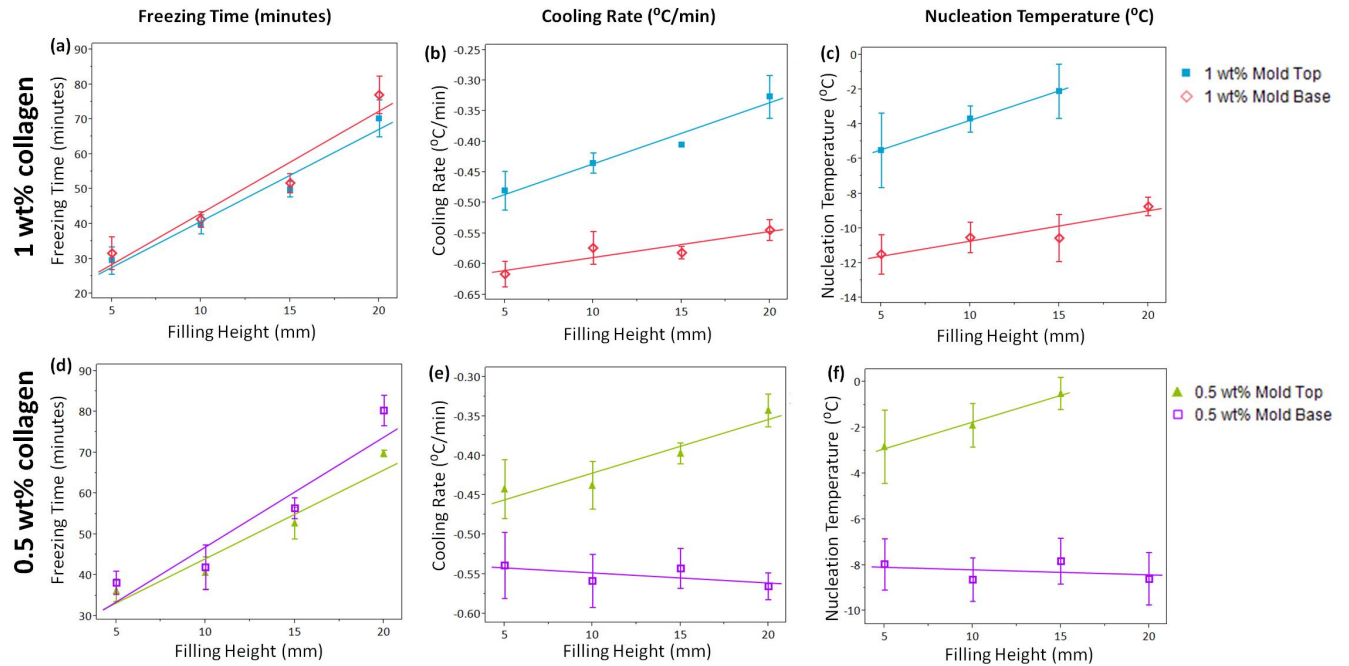


Figure 4: Relationship between filling height and thermal parameters in (a-c) 1 wt% collagen slurry and (d-f) 0.5wt% collagen slurry: (a, d) freezing time, (b, e) cooling rate of the slurry (c, f) nucleation temperature.

suspension, increased significantly as filling increased, Figure 4. Freezing time spanned a range of 30 - 70 minutes regardless of collagen weight percentage.

In contrast to freezing time, both the local cooling rate of the slurry and the nucleation temperature varied at the top and base. The cooling rate remained relatively constant at the base of the slurry, roughly -0.58 °C/min and -0.55 °C/min for 1 wt% and 0.5 wt% respectively. However, at the top of the scaffolds, the cooling rate decreased significantly as the filling increased from 5 to 20 mm. Values ranged from -0.48 to -0.33 for 1 wt% collagen slurry and from -0.44 to -0.34 °C/min for 0.5 wt% slurry.

The nucleation temperature followed the same trend as cooling rate. At the base, there was no significant difference in nucleation temperature with increased filling height, and the average nucleation temperature was -10.34 °C for 1 wt% slurry and -8.26 °C for 0.5 wt% slurry. At the top of the suspension, the nucleation temperature decreased systematically as filling height increased, Figure 4. In 1 wt% collagen slurry, the nucleation temperature at the top was reduced significantly from -5.5 to -2.1 °C as the filling increased from 5 mm to 15 mm. The same trend was observed in 0.5 wt% slurries, with a range of -2.83 to -0.5 °C. When the filling height reached 20 mm, no nucleation temperature was recorded at the top of the mold for either weight percent collagen.

3.3 Scaffold Architecture

As with the thermal parameters, as filling height increased, changes were observed in the pore structure of the scaffolds. Isotropic, equiaxed pores were observed at the base, regardless of filling height or collagen weight percentage. However, when the filling height reached 20 mm, isotropic, equiaxed pores at the base were replaced by anisotropic planes of pores at the top of the scaffolds, Figure 5. The aligned pores were oriented parallel to the thermal gradient within the slurry observed in the thermal profiles in Figure 3.

Pore size analysis revealed that pore size varied from 90 - 160 μm across 1 wt% collagen scaffolds. Scaffold pore size for 0.5wt% collagen scaffolds was significantly higher than scaffolds of 1 wt% collagen at both the top and base, between 120 - 170 μm . At the base of the scaffolds, where isotropic architecture was always present, the pore size remained constant regardless of filling height, 90 μm and 120 μm for 1 wt % and 0.5 wt% scaffolds respectively. In both cases, the pore size at the top of the mold increased significantly as filling increased, reaching a maximum pore size in 15 mm scaffolds, Figure 6. By 10 mm filling, the pore size at the top of scaffolds was significantly larger than the pore size at the base for both collagen concentrations. At 20 mm filling, the planes of pores were too anisotropic to compare to other pore size measurements.

4 Discussion

Effect of Filling Height on Thermal Parameters

As tissue engineering scaffolds seek to mimic specific tissue environments, the need to control scaffold structure becomes more and more relevant. Varying the filling height of collagen suspension produced systematic changes in thermal parameters. The insulating mold used during this study was designed to eliminate any temperature gradients except axial gradients, which could be controlled by varying the filling height. In this way, it was ensured that the point where the thermocouple recorded freezing behavior of the slurry was representative of the bulk at that height. The trends observed, which were quantified via thermal profiles, were consistent across collagen weight percentages, and thus representative of collagen scaffolds in general. It was found that latent heat release played a pivotal role in determining scaffold structure at the top of

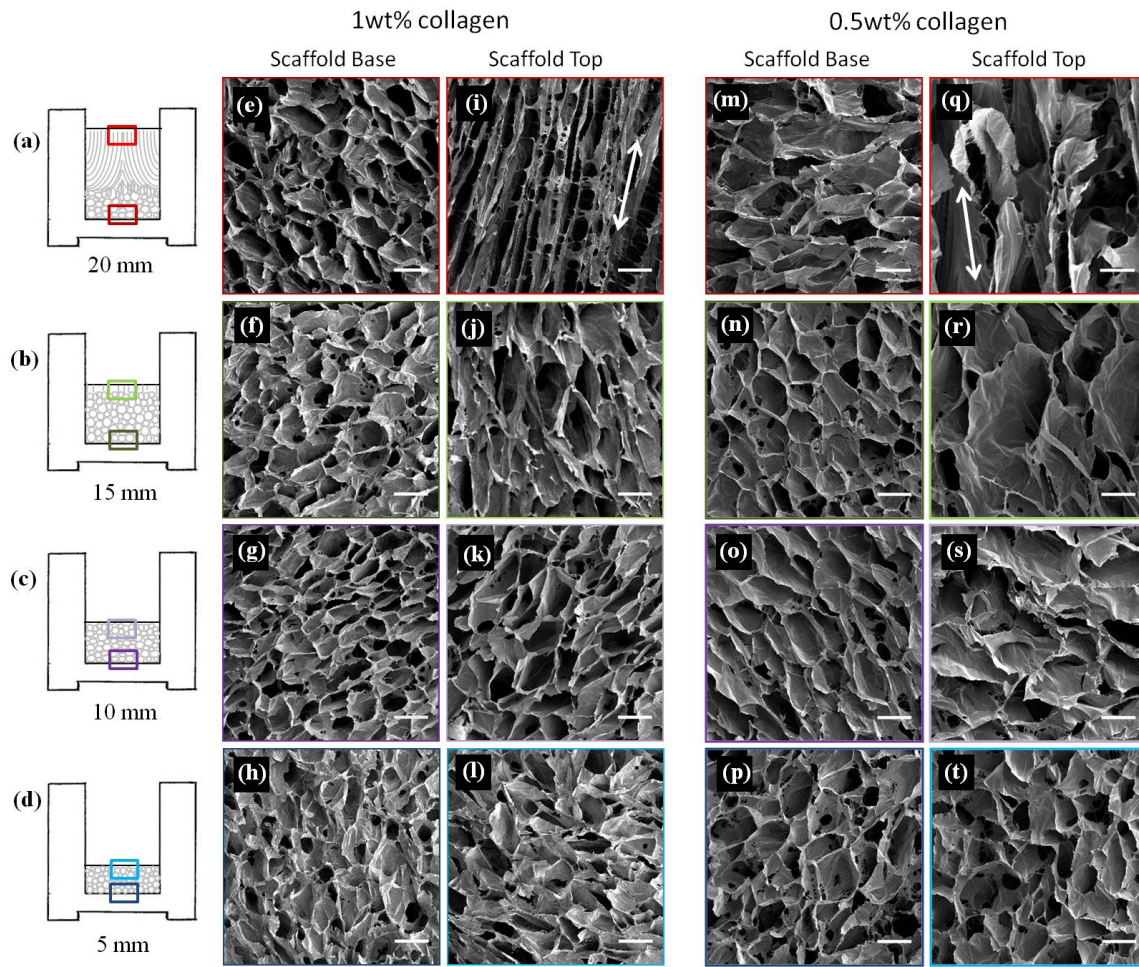


Figure 5: Micrographs of 1 wt% and 0.5 wt% freeze-dried collagen scaffold architecture at various filling heights: 5mm, 10 mm, 15mm, and 20 mm. (a-d) Schematics of scaffolds structure relative to the mold. Micrographs of 1 wt% collagen scaffolds at the (e-h) top and (i-l) base, and micrographs of 0.5 wt% scaffolds at the (m-p) top and (q-t) base. Scale bar is 200 μm in all images. White arrows mark the direction of axial porosity in anisotropic scaffold regions.

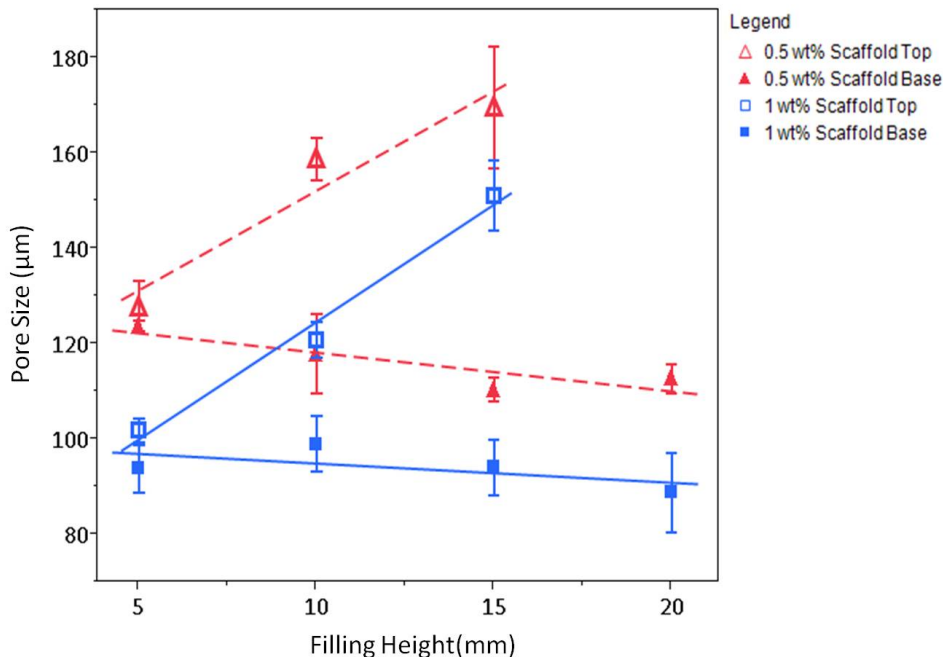


Figure 6: Pore size within 1 wt% and 0.5 wt% freeze dried collagen scaffolds varied between the top and base of the slurry. At the top of mold, pore size increased significantly with filling height, while remaining constant at the base of the mold. The average pore size increased significantly with lower weight percentages of collagen.

the mold by warming the slurry after nucleation began. From the profiles, primary nucleation occurred once within the slurry, and only in the portion of the slurry which was below the equilibrium freezing temperature. Latent heat release blocked any further stable nuclei from forming via primary nucleation at the top of the mold.

Within this study, as the volume of the slurry increased with filling height, freezing time also increased. Of all the parameters quantified, only freezing time did not vary at the top and base of the mold. Due to the relatively large thermal conductivity of the ice in the slurry, the latent heat produced during crystallization influences the temperature across the whole slurry. Hence the freezing temperature was not necessarily indicative of ongoing crystallization at the specific timepoint, but was tied to the removal of the latent heat produced during the crystallization process within the slurry. In literature, freezing time is linked to the amount of liquid which must still undergo solidification, and therefore continues to release latent heat, after the initial nucleation event [17]. Thus, at lower volumes, where a greater proportion of the liquid phase is converted to a solid upon nucleation, less crystal growth is required, resulting in shorter freezing time [6].

Local cooling rates were sensitive to filling height only at the top of the collagen slurries. During shelf-ramping freeze drying, heat conduction from the top of the suspension must occur through either the mold or the slurry itself. Given the thermally insulating nature of the perspex mold and the ice formed at the base of the mold, the greater the distance from the shelf, the more difficult heat conduction out of the slurry became. Thus, the cooling rate decreased as the filling height increased.

A consequence of the change in cooling rate at the top of the mold was the change in nucleation temperature with filling height. From the thermal profiles, the time at which nucleation occurred was dictated by the base of the mold. At the top of the mold, where heat removal was difficult, the nucleation temperature

was therefore dependent on how quickly the top of the slurry could cool. When the filling height increased sufficiently to 20 mm, the slurry at the top of the mold had not yet passed the equilibrium freezing temperature (0°C) and any solid which formed near the top quickly melted again. All of the initial solid formed at nucleation was therefore localized to a small volume at the base of the scaffold.

Anisotropic Scaffold Structure

The correlation between nucleation temperature and crystal structures has been noted previously. In a study on mannitol solutions, nucleation temperatures close to the equilibrium freezing temperature resulted in anisotropic crystal structures [18]. However, as the freezing profile was only recorded at the mid-point of the solutions, rather than, as in the present study, at both the top and base of the solution, it is likely that in [Nakagawa ref] the nucleation temperature at the top of the solution was above the equilibrium freezing temperature when the base of the solution nucleated [18]. The anisotropic, lamellar architecture which was observed within this study developed from ice crystals at the base growing upwards into the liquid slurry as it cooled. The orientation of the lamellar structure parallel to temperature gradient, dominates due to a number of factors including anisotropic growth of ice crystals, efficiency of solute exclusion from each crystal orientation, and the nature of the external thermal gradients [19].

Changes in architecture with cooling rate are not uncommon, especially at very high cooling rates, such as during liquid nitrogen quenching [14, 20]. Ice has a natural inclination to form dendrites, and anisotropic scaffolds have been previously observed [21]. However, liquid nitrogen quenching is not always necessary to produce aligned scaffolds, as long as the cooling rate is sufficiently high [22]. Scaffolds have been demonstrated to shift from equiaxed pore structures to aligned porosity as the set cooling rate decreased from -0.83°C/min to over - 20°C/min [14].

We have demonstrated that a high cooling rate is not vital to creating axially aligned porosity, but that a large difference in cooling rates within the liquid is necessary so that the temperature at the slurry top can not reach equilibrium temperature at nucleation. Thus, even though the cooling rates of the slurry in this study did not exceed -0.6 °C/min, anisotropic scaffold architecture still resulted. Monitoring the local nucleation temperature is therefore key to predicting anisotropy within collagen scaffolds regardless of slurry concentration or the external set cooling rate.

Pore Size and Filling Height

Even within isotropic scaffolds, pore size at the top of the scaffolds was affected by filling height. This phenomenon has been reported in previous literature in systems using mannitol solutions, suggesting that it is a general property of ice crystallization and growth during freezing [18, 23, 6].

The largest pore size was reported at the top of scaffolds with 15 mm filling. At this point, the nucleation temperature was very close to the equilibrium temperature, suggesting that 15 mm was close to the maximum filling which could be achieved before anisotropic architecture would result. Pore sizes ranged from 90 - 170 μm , which is well above the reported lower limit for cell culture of 10 - 50 μm in diameter [24]. There appeared to be a lower limit on the pore size within scaffolds, which occurred at around 90-100 μm , a phenomenon which has been previously reported and attributed to the limiting effect of the glass transition temperature on diffusion within a collagen suspension [12]. Scaffolds of 0.5 wt% collagen had significantly larger pore sizes than in 1 wt% scaffolds, in agreement with literature, and most likely results from the lower number of heterogeneous nucleation sites within the slurry with decreased collagen content [25, 26].

General Principles

While our findings are based on the ice templating of collagen suspensions, the use of directional freezing to create ice templates can be applied to a broad variety of materials systems, including synthetic polymers, pharmaceutical drugs, and ceramics [18, 27, 28]. An important step in designing scaffolds with specific architecture, is understanding the interplay between thermal variables of the suspension, such as nucleation temperature, local cooling rate, and filling of the mold in freeze drying systems. While on-going pharmaceutical research has been conducted on this subject for a number of years, the way in which thermal parameters influence porous scaffold morphology is largely unexplored [8, 29]. Most studies have investigated how changes in processing variables, such as set freezing temperature or set cooling rate relate to pore structure. It was only relatively recently that various groups began recording the internal temperature changes within freezing collagen slurries which result in structural changes [11, 12]. Within this study, changes to the local nucleation temperature, mediated by the local cooling rate, were found to be key to the formation of anisotropic scaffolds. Thus, it was critical to monitor the local thermal behavior of the slurry to understand how anisotropic ice templating occurs. As the cooling rate of slurry throughout the sample is tied to the ability to remove latent heat, mold design is an important consideration for creating architecture and controlling nucleation.

5 Conclusions

Local thermal parameters were found to control the scaffold structure during ice templating. The release of latent heat after primary nucleation, which could not be removed quickly. Subsequently blocked further nucleation from occurring. As a consequence, anisotropic scaffold structures occurred when the nucleation temperature at the top of the mold was above the equilibrium freezing temperature (0 °C) of the slurry. In turn, the nucleation temperature at the mold top was influenced by the local cooling rate. Changing the weight percentage of collagen within slurries did not affect the trends in local thermal parameters, or the shift from isotropic to anisotropic porosity. As so much depends on the removal of heat within molds, future work will concentrate on using mold design to control the thermal conduction during freeze drying and thus, scaffold architecture.

6 Acknowledgements

The authors gratefully acknowledge the financial support of the Gates Cambridge Trust, the Newton Trust, and ERC. A.H. holds a Daphne Jackson Fellowship funded by the University of Cambridge.

References

- [1] M. E. Kolewe, H. Park, C. Gray, X. Ye, R. Langer, and L. E. Freed, “3d structural patterns in scalable, elastomeric scaffolds guide engineered tissue architecture,” *Advanced Materials* doi: [10.1002/adma.201301016](https://doi.org/10.1002/adma.201301016), 2013.
- [2] H. X. Lu, Y. G. Ko, N. Kawazoe, and G. P. Chen, “Cartilage tissue engineering using funnel-like collagen sponges prepared with embossing ice particulate templates,” *Biomaterials* **31**(22), pp. 5825–5835, 2010.

- [3] M. J. W. Koens, P. J. Geutjes, K. A. Faraj, J. Hilborn, W. F. Daamen, and T. H. van Kuppevelt, "Organ-specific tubular and collagen-based composite scaffolds," *Tissue Engineering Part C-Methods* **17**(3), pp. 327–335, 2011.
- [4] K. A. Faraj, T. H. Van Kuppevelt, and W. F. Daamen, "Construction of collagen scaffolds that mimic the three-dimensional architecture of specific tissues," *Tissue Engineering* **13**(10), pp. 2387–2394, 2007.
- [5] H. Schoof, J. Apel, I. Heschel, and G. Rau, "Control of pore structure and size in freeze-dried collagen sponges," *Journal of Biomedical Materials Research* **58**(4), pp. 352–357, 2001.
- [6] A. Hottot, S. Vessot, and J. Andrieu, "Freeze drying of pharmaceuticals in vials: Influence of freezing protocol and sample configuration on ice morphology and freeze-dried cake texture," *Chemical Engineering and Processing* **46**(7), pp. 666–674, 2007.
- [7] J. Searles, "Freezing and annealing phenomena in lyophilization," in *Freeze-Drying/Lyophilization of Pharmaceutical and Biological Products*, L. Rey and J. May, eds., ch. 4, Marcel Dekker, Inc., New York, 2nd ed., 2004.
- [8] J. A. Searles, J. F. Carpenter, and T. W. Randolph, "The ice nucleation temperature determines the primary drying rate of lyophilization for samples frozen on a temperature-controlled shelf," *Journal of Pharmaceutical Sciences* **90**(7), pp. 860–871, 2001.
- [9] M. Akyurt, G. Zaki, and B. Habeebullah, "Freezing phenomena in ice-water systems," *Energy Conversion and Management* **43**(14), pp. 1773–1789, 2002.
- [10] A. Myerson and G. R., "Crystals, crystal growth and nucleation," in *Handbook of Industrial Crystallization*, A. Myerson, ed., ch. 2, pp. 33–62, Butterworth-Heinemann, 2nd ed., 2002.
- [11] F. J. O'Brien, B. A. Harley, I. V. Yannas, and L. J. Gibson, "The effect of pore size on cell adhesion in collagen-gag scaffolds," *Biomaterials* **26**(4), pp. 433–441, 2005.
- [12] M. G. Haugh, C. M. Murphy, and F. J. O'Brien, "Novel freeze-drying methods to produce a range of collagen-glycosaminoglycan scaffolds with tailored mean pore sizes," *Tissue Engineering Part C-Methods* **16**(5), pp. 887–894, 2010.
- [13] F. J. O'Brien, B. A. Harley, I. V. Yannas, and L. Gibson, "Influence of freezing rate on pore structure in freeze-dried collagen-gag scaffolds," *Biomaterials* **25**(6), pp. 1077–1086, 2004.
- [14] N. Y. Yuan, Y. A. Lin, M. H. Ho, D. M. Wang, J. Y. Lai, and H. J. Hsieh, "Effects of the cooling mode on the structure and strength of porous scaffolds made of chitosan, alginate, and carboxymethyl cellulose by the freeze-gelation method," *Carbohydrate Polymers* **78**(2), pp. 349–356, 2009.
- [15] J. Lim, J. Kim, K. Yu, E. Lim, S. Lee, and G. Park, "Heat pulse method for thermal diffusivity measurements of pvdf/pmma blends," *Journal of the Korean Physical Society* **32**, pp. S228–S231, 1998.
- [16] D. W. James, "The thermal diffusivity of ice and water between -40 and +60 degrees c," *Journal of Materials Science* **3**(5), pp. 540–543, 1968.
- [17] X. L. Tang and M. J. Pikal, "Design of freeze-drying processes for pharmaceuticals: Practical advice," *Pharmaceutical Research* **21**(2), pp. 191–200, 2004.

- [18] K. Nakagawa, A. Hottot, S. Vessot, and J. Andrieu, "Influence of controlled nucleation by ultrasounds on ice morphology of frozen formulations for pharmaceutical proteins freeze-drying," *Chemical Engineering and Processing* **45**(9), pp. 783–791, 2006. Times Cited: 33 34.
- [19] S. Deville, E. Maire, A. Lasalle, A. Bogner, C. Gauthier, J. Leloup, and C. Guizard, "In situ x-ray radiography and tomography observations of the solidification of aqueous alumina particle suspensions-part i: Initial instants," *Journal of the American Ceramic Society* **92**(11), pp. 2489–2496, 2009.
- [20] F. Burette, F. Bouchard, C. Pellerin, J. Paquin, I. Marcotte, and M. A. Mateescu, "Cell-culture compatible silk fibroin scaffolds concomitantly patterned by freezing conditions and salt concentration," *Polymer Bulletin* **67**(1), pp. 159–175, 2011.
- [21] H. Schoof, L. Bruns, A. Fischer, I. Heschel, and G. Rau, "Dendritic ice morphology in unidirectionally solidified collagen suspensions," *Journal of Crystal Growth* **209**(1), pp. 122–129, 2000.
- [22] J. A. Searles, J. F. Carpenter, and T. W. Randolph, "Annealing to optimize the primary drying rate, reduce freezing-induced drying rate heterogeneity, and determine t-g' in pharmaceutical lyophilization," *Journal of Pharmaceutical Sciences* **90**(7), pp. 872–887, 2001.
- [23] K. Nakagawa, A. Hottot, S. Vessot, and J. Andrieu, "Modeling of freezing step during freeze-drying of drugs in vials," *Aiche Journal* **53**(5), pp. 1362–1372, 2007.
- [24] B. Harley and I. Yannas, "In vivo synthesis of tissues and organs," in *Principles of Tissue Engineering*, R. Lanza, R. Langer, and J. Vacanti, eds., ch. 16, pp. 219–238, Elsevier Academic Press, New York, 3rd ed., 2007.
- [25] M. Madaghiele, A. Sannino, I. V. Yannas, and M. Spector, "Collagen-based matrices with axially oriented pores," *Journal of Biomedical Materials Research Part A* **85A**(3), pp. 757–767, 2008.
- [26] M. C. Gutierrez, M. L. Ferrer, and F. del Monte, "Ice-templated materials: Sophisticated structures exhibiting enhanced functionalities obtained after unidirectional freezing and ice-segregation-induced self-assembly," *Chemistry of Materials* **20**(3), pp. 3505–3513, 2008.
- [27] H. Zhang and A. I. Cooper, "Aligned porous structures by directional freezing," *Advanced Materials* **19**(11), pp. 1529–1533, 2007.
- [28] S. Deville, E. Saiz, and A. P. Tomsia, "Freeze casting of hydroxyapatite scaffolds for bone tissue engineering," *Biomaterials* **27**(32), pp. 5480–5489, 2006.
- [29] J. Andrieu, A. Hottot, and S. Vessot, "Freeze drying of pharmaceuticals in vials: Influence of freezing protocol and sample configuration on ice morphology and freeze-dried cake texture," *Chemical Engineering and Processing* **46**(7), pp. 666–674, 2007.